Electronic Supplementary Material

Encapsulating segment-like antimony nanorod in hollow carbon tube as long-lifespan, high-rate anodes for rechargeable K-ion batteries

Wen Luo[1,§], Feng Li[2,§], Weiran Zhang[3], Kang Han[4], Jean-Jacques Gaumet[5], Hans-Eckhardt Schaefer[4,6], and Liqiang Mai[4] (✉)

[1] *Department of Physics, School of Science, Wuhan University of Technology, Wuhan 430070, China*
[2] *Hefei National Laboratory for Physical Sciences at the Microscale, University of Science and Technology of China, Hefei 230000, China*
[3] *Division of Materials Science and Engineering, Boston University, MA 02215, USA*
[4] *State Key Laboratory of Advanced Technology for Materials Synthesis and Processing, International School of Materials Science and Technology, Wuhan University of Technology, Wuhan 430070, China*
[5] *Laboratoire de Chimie et Physique: Approche Multi-échelles des Milieux Complexes, Institut Jean Barriol, Université de Lorraine, Metz 57070, France*
[6] *Institute for Functional Matter and Quantum Technologies, Stuttgart University, Pfaffenwaldring 57, Stuttgart 70569, Germany*
[§] *Wen Luo and Feng Li contributed equally to this work.*

Supporting information to https://doi.org/10.1007/s12274-019-2335-6

I Materials and Methods

All the reagents used in the experiment were of analytical grade and used without further purification.

Synthesis of Sb_2S_3 nanorods. The Sb_2S_3 nanorods were obtained by a simple hydrothermal method referring to a previous report[1]. In details, 4 mmol $SbCl_3$, 8 mmol $C_3H_7NO_2S$ (L-cysteine), and 8 mmol $Na_2S \cdot H_2O$ were orderly dissolved in 80 mL deionized water with constant stirring for 3 h at room temperature, then the mixture was transferred into 100 mL Teflon-lined autoclave and kept at 180 °C for 12 h. After cooling down to room temperature, the black product, Sb_2S_3 nanorods were collected by centrifugation and washed by deionized water and ethanol for several times. Finally the product was obtained after drying in a vacuum oven at 70 °C overnight.

Synthesis of Sb_2S_3@PPy nanorods. 80 mg as-prepared Sb_2S_3 nanorods , 4 mg sodium dodecyl sulfate (SDS) was dissolved into 40 mL deionized water with sonication for 0.5 h and then under stirring for another 1 h. In the following step, 21 μL pyyrole monomer (py) was added into the above suspension with further constant stirring for 1 h. Then 4 mL $(NH_4)_2S_2O_8$ solution (0.1 M in deionized water) was dropwise added into above suspension. The mixture was stirring for 4 h at room temperature. Sb_2S_3@PPy nanorods were collected by centrifugation and washed by deionized water and ethanol for several times and finally were obtained by freeze-drying process overnight.

Synthesis of Sb@HCT nanorods. Sb_2S_3@PPy nanorods can be transformed to peapod-like Sb@HCT nanorods after high-temperature calcination and reduction for 45 min at 450 ℃ with a heating rate of 3 °C min^{-1} under H_2/Ar (5% : 95%, volume ratio). Time independent experiments was taken to explore its high temperature pyrolysis reduction mechanism. Specifically, bare Sb_2S_3 and Sb_2S_3@PPy nanorods were calcined at 450 °C for 5, 15, 30, 45, 60, and 75 min, respectively, then cooling down to room temperature.

Materials characterization. The micro-nano structure, morphology and element information of above samples were acquired from JEOL-7100F scanning electron microscope (SEM)/energy dispersive spectroscopy (EDS) at an acceleration voltage of 20 kV and JEM-2100F STEM/EDS microscope. The crystal structure of samples and cycled electrodes with different status was characterized by Bruker D8 Advance X-ray diffractometer with a nonmonochromated Cu Kα X-ray source. XPS was collected from VG Multi Lab 2000 instrument. TG/DSC was performed using a Netzsch STA 449C simultaneous thermal analyzer at a heating rate of 10 °C min^{-1} in air atomsphere. Raman spectra were collected through a Renishaw inVia Raman microscope. A 633 or 532 nm He-Ne laser was focused on the samples for different test conditions.

Electrochemical performance measurement. The potassium storage performance of Sb@HCT was tested by the assembling of potassium half cell (CR-2016). Electrodes were produced from a slurry by the mixture of Sb@HCT, ketjen black and carboxyl methyl cellulose at a mass ratio of 70:20:10. The slurry was pasted on copper foil and dried at 70 °C in an oven overnight. The average mass loading of the active material was around 1.2 mg cm^{-2}. Then the half cells was fabricated in a glove box filled with pure argon using potassium metal as counter electrode. The electrolyte were prepared by dissolving 1.0 M KPF_6 or 1.0 M KFSI in ethylene carbon (EC)/dimethyl carbonate (DMC) (1:1 vol/vol), respectively. The Whatman glass fiber membrane (GF/D) was used as the separator. The electrochemical performance of Sb@HCT can be attained at the voltage range of 0.01–3.0 V from Land CT2001A battery testing system. Cyclic voltammetry (CV) curves were conducted from 0.01 to 3.0 V versus K/K^+ on an electrochemical workstation at scan rates of 0.2 mV s^{-1} (Autolab PGSTAT 302). Electrochemical impedance spectroscopy (EIS) measurements were performed on an Autolab PGSTAT 302N electrochemical workstation over the frequency range of 100 kHz–0.01 Hz. All the electrochemical tests were conducted at room temperature.

Address correspondence to mlq518@whut.edu.cn

II Supplementary Figures

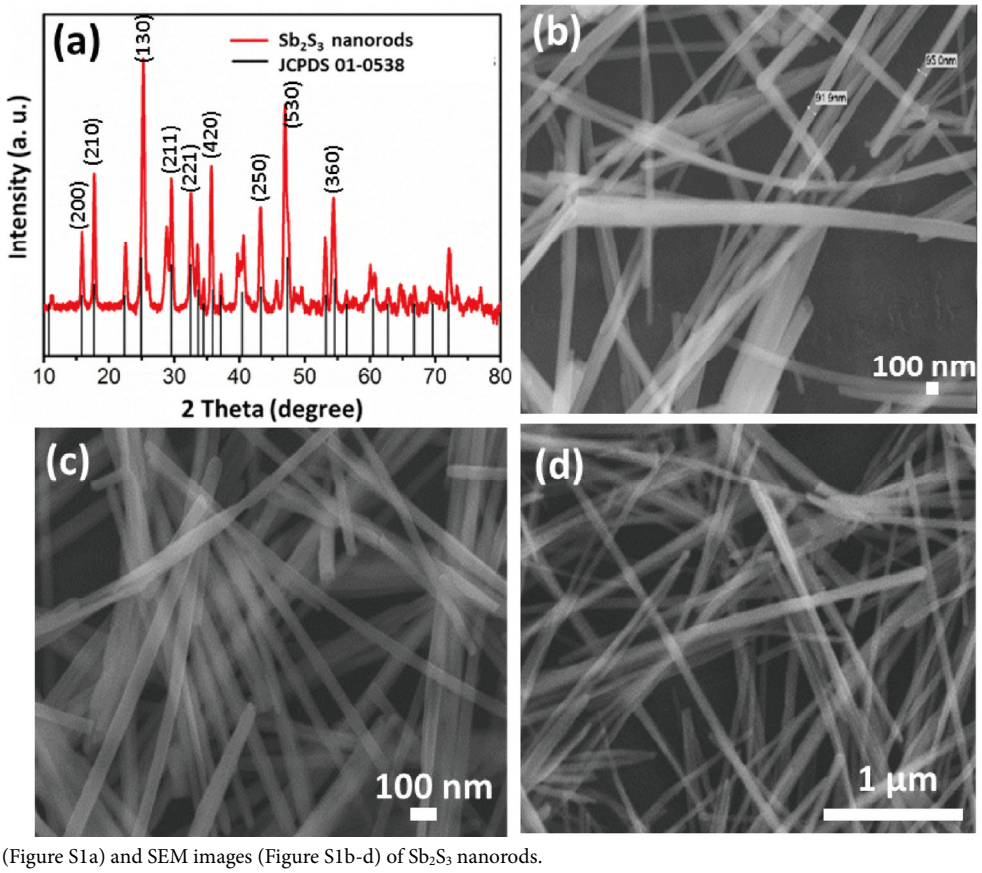

Figure S1 XRD pattern (Figure S1a) and SEM images (Figure S1b-d) of Sb_2S_3 nanorods.

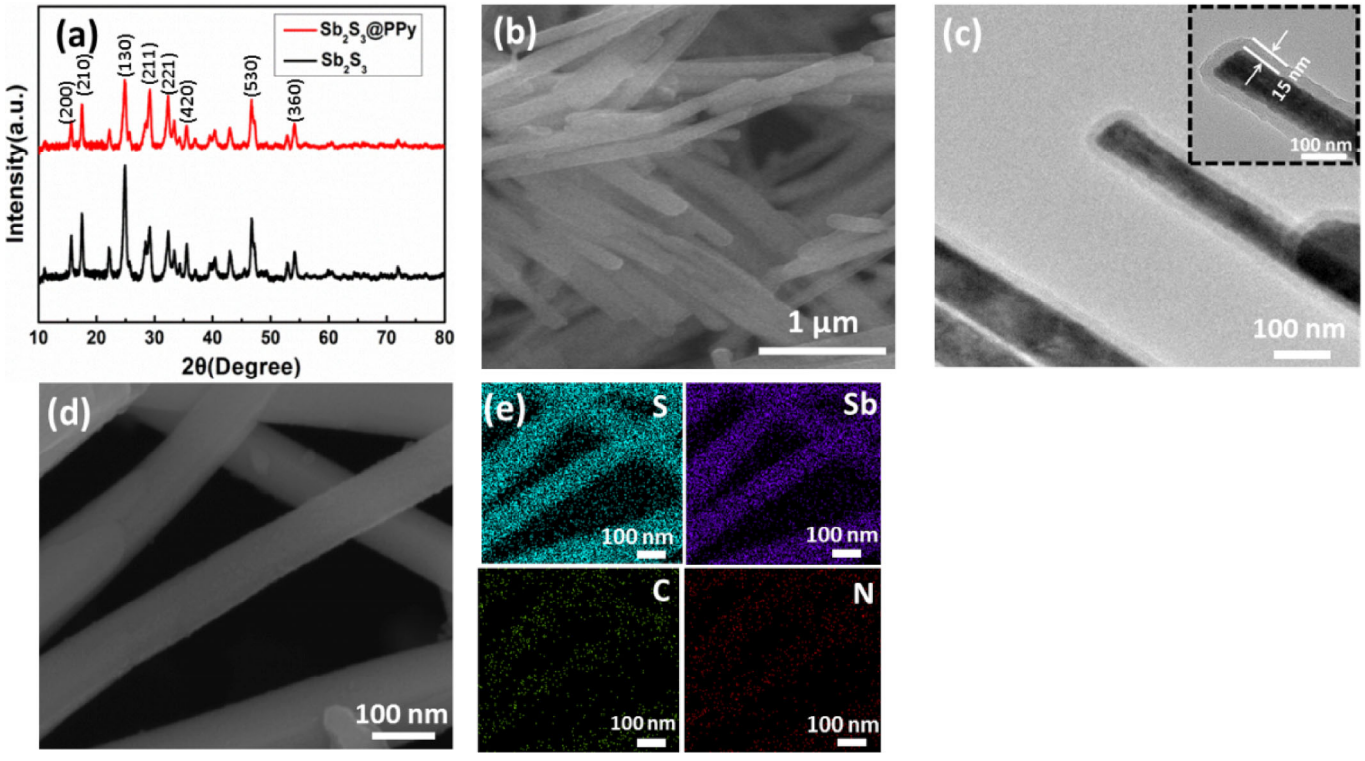

Figure S2 XRD pattern (Figure S2a), SEM image (Figure S2b), TEM image (Figure S2c) and SEM image (Figure S2d) and corresponding elemental mapping (Figure S2e) of Sb_2S_3@PPy nanorods.

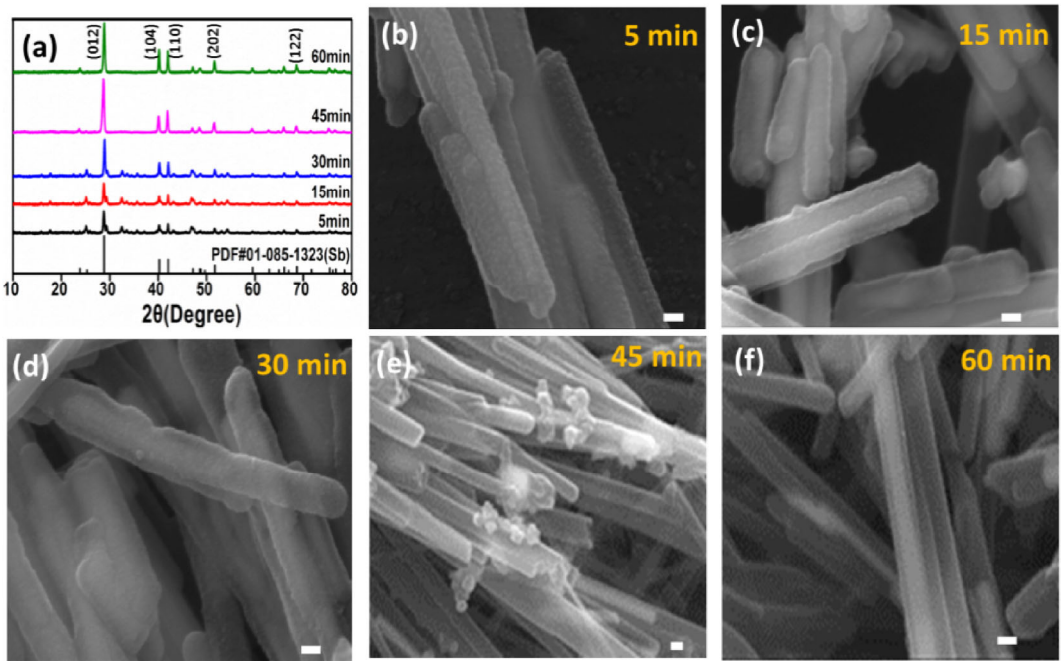

Figure S3 XRD patterns (Figure S3a) and SEM images (Figure S3b-f) of calcined Sb_2S_3@PPy nanorods at different times, namely 5 (Figure S3b), 15 (Figure S3c), 30 (Figure S3d), 45 (Figure S3e) and 60 min (Figure S3f). *Scale bar in Figure S3b-f: 100 nm*.

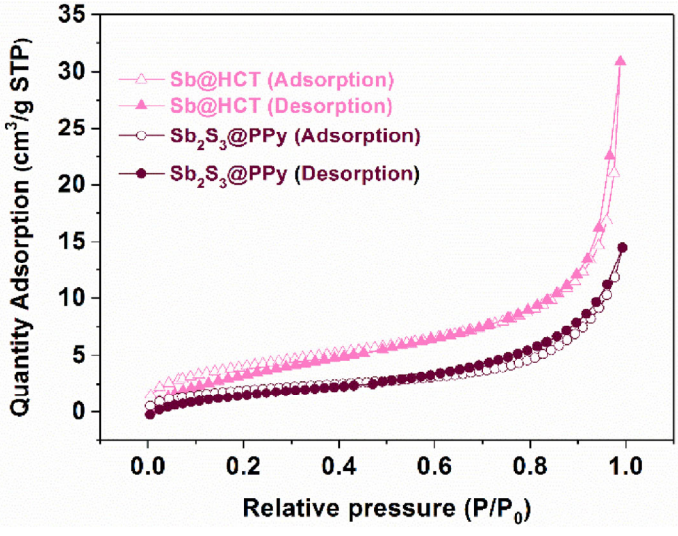

Figure S4 Nitrogen adsorption curves of Sb_2S_3@PPy nanorods and Sb@HCT.

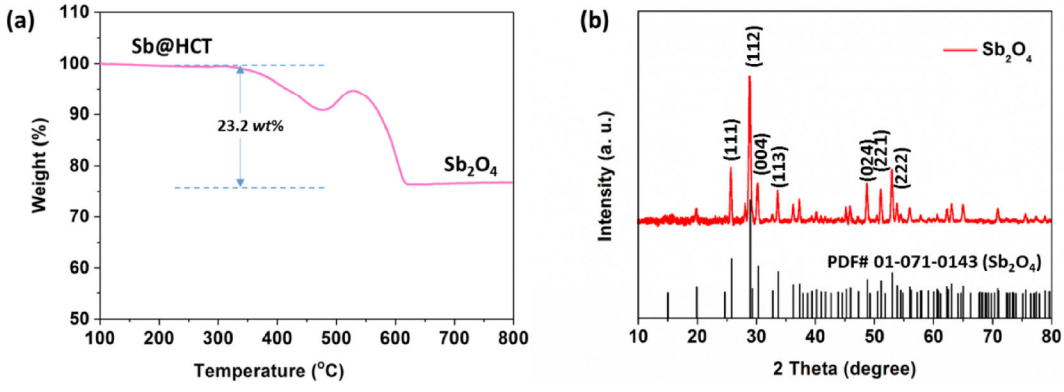

Figure S5 (a) TGA curve of Sb@HCT; (b) XRD pattern of the combustion product of Sb@HCT. The total Sb content in the composite was calculated based on the following equation:

$$\mathrm{Sb\,(wt\%)} = 100 * \frac{\text{molecular weight of Sb}}{\text{molecular weight of } Sb_2O_4} * \frac{\text{final weight of } Sb_2O_4}{\text{initial weight of Sb@HCT}}$$

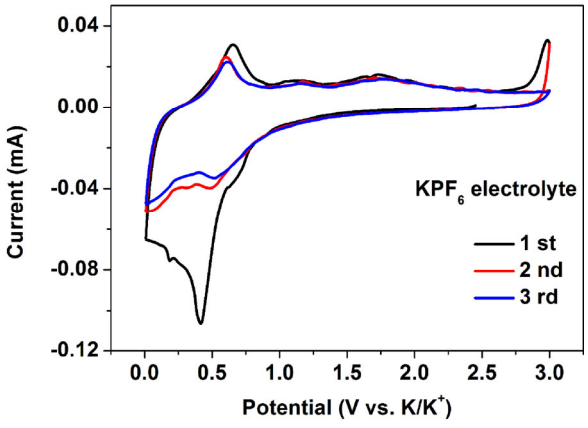

Figure S6 The first three CV curves of Sb@HCT in the KPF_6 electrolyte at a scan rate of 0.2 mV s^{-1}.

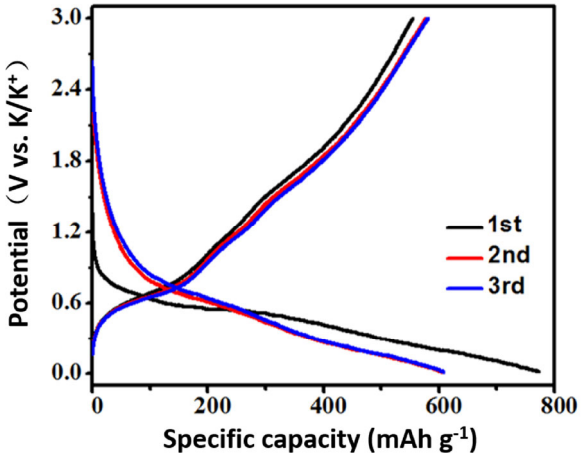

Figure S7 Typical charge/discharge curves of Sb@HCT anode in KFSI electrolyte for the first three cycles at a current density of 0.5 A g^{-1}.

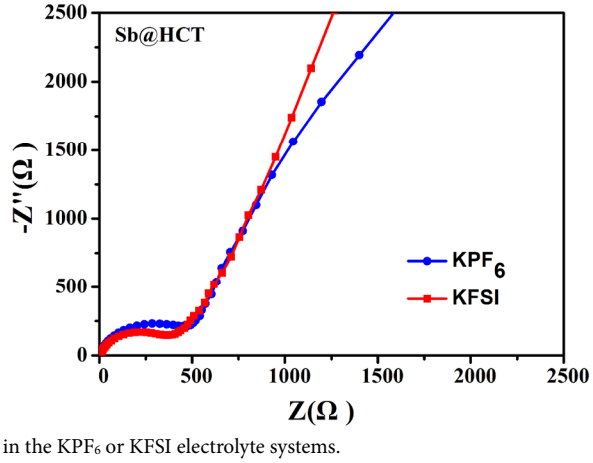

Figure S8 Nyquist plots of Sb@HCT electrode in the KPF_6 or KFSI electrolyte systems.

Table S1 Comparison of electrochemical performances of alloying or conversion based anodes for KIB

Representative anodes	Cycling performance	Rate capability	Ref.
SnS_2-rGO	280 mAh·g^{-1} after 25 cycles at 25 mA g^{-1}	120 mAh·g^{-1} at 2 A g^{-1}	[2]
Sn/C	150 mAh·g^{-1} after 30 cycles at 25 mA g^{-1}	/	[3]
Sb@3D-C composite	225 mAh·g^{-1} after 50 cycles at 1000 mA g^{-1}	288 mAh·g^{-1} at 1 A g^{-1}	[4]
Sn_4P_3/C	307 mAh·g^{-1} after 50 cycles at 50 mA g^{-1}	221.9 mAh·g^{-1} at 1 A g^{-1}	[5]
CoS/graphene	310.8 mAh·g^{-1} after 100 cycles at 500 mA g^{-1}	210 mAh·g^{-1} at 2 A g^{-1}	[6]
Black phosphorus	270 mAh·g^{-1} after 50 cycles at 500 mA g^{-1}	280 mAh·g^{-1} at 2 A g^{-1}	[7]
Porous Bi	322 mAh·g^{-1} after 300 cycles at 770 mA g^{-1}	321.9 mAh·g^{-1} at 1.15 A g^{-1}	[8]
Bi/rGO	290 mAh·g^{-1} after 50 cycles at 50 mA g^{-1}	235 mAh·g^{-1} at 0.5A g^{-1}	[9]
Sb@HCT	300.1 mAh·g^{-1} after 120 cycles at 2,000 mA g^{-1}	211.5 mAh·g^{-1} at 5A g^{-1}	Present work

References

[1] N. Wang, Z. Bai, Y. Qian, J. Yang, Adv. Mater. 28 (2016) 4126-4133.
[2] V. Lakshmi, Y. Chen, A. A. Mikhaylov, A. G. Medvedev, I. Sultana, M. M. Rahman, O. Lev, P. V. Prikhodchenko, A. M. Glushenkov, Chem. Commun. 53 (2017) 8272-8275.
[3] I. Sultana, T. Ramireddy, M. M. Rahman, Y. Chen, A. M. Glushenkov, Chem. Commun. 52 (2016) 9279-9282.
[4] C. Han, K. Han, X. Wang, C. Wang, Q. Li, J. Meng, X. Xu, Q. He, W. Luo, L. Wu, Nanoscale 10 (2018) 6820-6826.
[5] W. Zhang, J. Mao, S. Li, Z. Chen, Z. Guo, J Am. Chem. Soc. 139 (2017) 3316-3319.
[6] H. Gao, T. Zhou, Y. Zheng, Q. Zhang, Y. Liu, J. Chen, H. Liu, Z. Guo, Adv. Funct. Mater. 27 (2017) 1702634.
[7] I. Sultana, M. M. Rahman, T. Ramireddy, Y. Chen, A. M. Glushenkov, J Mater. Chem. A 5 (2017) 23506-23512.
[8] K. Lei, C. Wang, L. Liu, Y. Luo, C. Mu, F. Li, J. Chen, Angewandte Chemie 130 (2018) 4687-4691.
[9] Q. Zhang, J. Mao, W. K. Pang, T. Zheng, V. Sencadas, Y. Chen, Y. Liu, Z. Guo, Adv. Energy Mater. (2018) 1703288.